DOI: 10.1002/chem.200800369

Synthesis, Surface Modifications, and Size-Sorting of Mixed Nickel–Zinc Ferrite Colloidal Magnetic Nanoparticles

P. Majewski and P. Krysiński*[a]

Abstract: We report on the spontaneous covalent growth of monomolecular adlayers on mixed nickel–zinc nanoferrite colloidal suspensions (ferrofluids). Synthesized nanoparticles were subjected to surface modification by means of acid chloride chemistry, leading to the formation of covalent bonds between the hydroxy groups at the nanoparticle surface and the acid chloride molecules. This procedure can be easily tailored to allow for the formation of adlayers containing both hydrophobic and hydrophilic regions stacked at predetermined distances from the magnetic core, and also providing the nanoferrites with functional carboxy groups capable of further modifications with, for example, drug molecules. Here, fluorophore aminopyrene molecules were bound to such modified nanoferrites through amide bonds. We also used the same chemistry to modify the surface with covalently bound long-chain palmitoyl moieties, and for comparison we also modified the nanoferrite surface by simple adsorption of oleic acid. Both procedures made the surface highly hydrophobic. These hydrophobic colloids were subsequently spread on an aqueous surface to form Langmuir monolayers with different characteristics. Moreover, since uniformity of size is crucial in a number of applications, we propose an efficient way of sorting the magnetic nanoparticles by size in their colloidal suspension. The suspension is centrifuged at increasing rotational speed and the fractions are collected after each run. The mean size of nanoferrite in each fraction was measured by the powder X-ray diffraction (PXRD) technique.

Keywords: ferrofluids · Langmuir films · magnetic nanoparticles · nanoferrites · surface chemistry

Introduction

Magnetic ferrite nanoparticles are a recent key topic in modern science and biotechnology, due to their unique properties, which give them a variety of possible applications. These include both technological[1–4] and biological and medical applications, such as contrast increase of MRI and targeted drug delivery.[5–10] Our previous work on the covalent attachment of molecular adlayers to a variety of surfaces has shown that simple displacement reactions can be used on essentially any surface where hydroxy groups are present. We have attached molecular layers covalently to silica, indium tin oxide (ITO), boron-doped diamond, and electrochemically generated gold oxide surfaces by allowing the surface hydroxy groups to react with acid chlorides.[11–13]

Here we report on the covalent attachment of monomolecular adlayers to mixed nickel–zinc nanoferrite surfaces. Synthesized nanoparticles were subjected to surface modification by means of acid chloride chemistry, leading to the formation of covalent bonds between the hydroxy groups on the nanoparticle surface and the acid chloride molecules. In this paper we have used adipoyl and sebacoyl chlorides to functionalize the surfaces of nanoferrites. This procedure can be easily tailored to allow for the formation of adlayers containing both hydrophobic and hydrophilic regions stacked at predetermined distances from the magnetic core, also providing the colloidal nanoferrites with functional carboxy groups capable of further modifications with, for example, drug molecules. Here, fluorophore aminopyrene molecules were bound to such modified nanoferrites through amide bonds, and their steady-state fluorescence spectra were recorded, verifying the fluorophore attachment.

We also used the same chemistry to modify the surfaces with covalently bound long-chain palmitoyl moieties, and for comparison we also modified the nanoferrite surface by simple adsorption of oleic acid. Both procedures made the surfaces highly hydrophobic. These hydrophobic, sterically stabilized colloids were subsequently spread on aqueous surfaces to form Langmuir monolayers with totally different characteristics.

[a] P. Majewski, Prof. Dr. P. Krysiński
Laboratory of Electrochemistry, Department of Chemistry
University of Warsaw, 02-093 Warsaw, Pasteura 1 (Poland)
Fax: (+48) 22 8225996
E-mail: pakrys@chem.uw.edu.pl

Colloidal ferrites are usually synthesized in a relatively simple aqueous precipitation reaction,[14,15] which can be easily adapted for large-scale preparations. However, the main disadvantage of this route is the relatively high polydispersity of the resultant product, which is unsatisfactory for a number of practical applications, particularly where high electromagnetic permeability and low energy losses are required.[19] Therefore, in this work we also propose an efficient way of sorting nanoferrite particles by size. A colloidal suspension of nanoparticles is centrifuged at increasing rotational speed, and the fraction sedimented on the bottom of the centrifuge tube is collected after each run. Quantitatively, the mean size of nanoferrites in each fraction is measured by the powder X-ray diffraction (PXRD) technique.

Results and discussion

Crystallography of mixed $Ni_{0.5}Zn_{0.5}Fe_2O_4$ ferrites: In order to verify the mixed nature of $Ni_{0.5}Zn_{0.5}Fe_2O_4$ ferrofluid we performed PXRD experiments with unsorted, dry solid samples of obtained product. The diffraction patterns are shown in Figure 1.

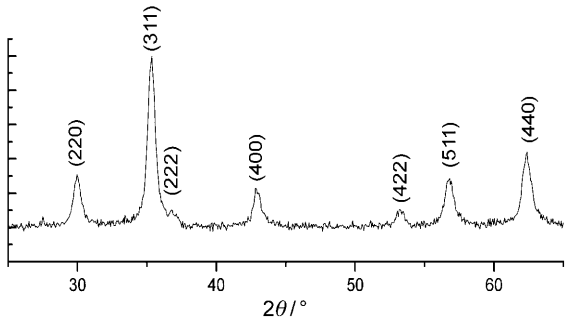

Figure 1. PXRD reflection patterns (indexed) of mixed nickel–zinc nanoferrites.

Analysis of the indexed pattern confirmed the crystallographic regular (space group 227—*Fd*3*m*) structure of nickel–zinc ferrite. Full width at half maximum (FWMH) values of six reflections shown on the PXRD pattern were used to evaluate the mean diameters of unsorted nanoparticles, according to the Scherrer equation,[16] with the assumption of spherical shapes for the ferrite nanoparticles. This procedure yielded (14 ± 1) nm as a mean particle radius, a value in good agreement with results obtained in the literature.[17,18]

To address the chemical compositions of obtained ferrofluids we performed PXRD experiments for ferrites of known Ni/Zn ratios, obtained by thermal (1100 °C, 2 h) decomposition of precursor mixtures of appropriate metal nitrates. For the series of ferrite nanoparticles differing in Ni/Zn ratio we observed a shift of X-ray reflections towards larger angles with increasing zinc content, as shown in Figure 2.

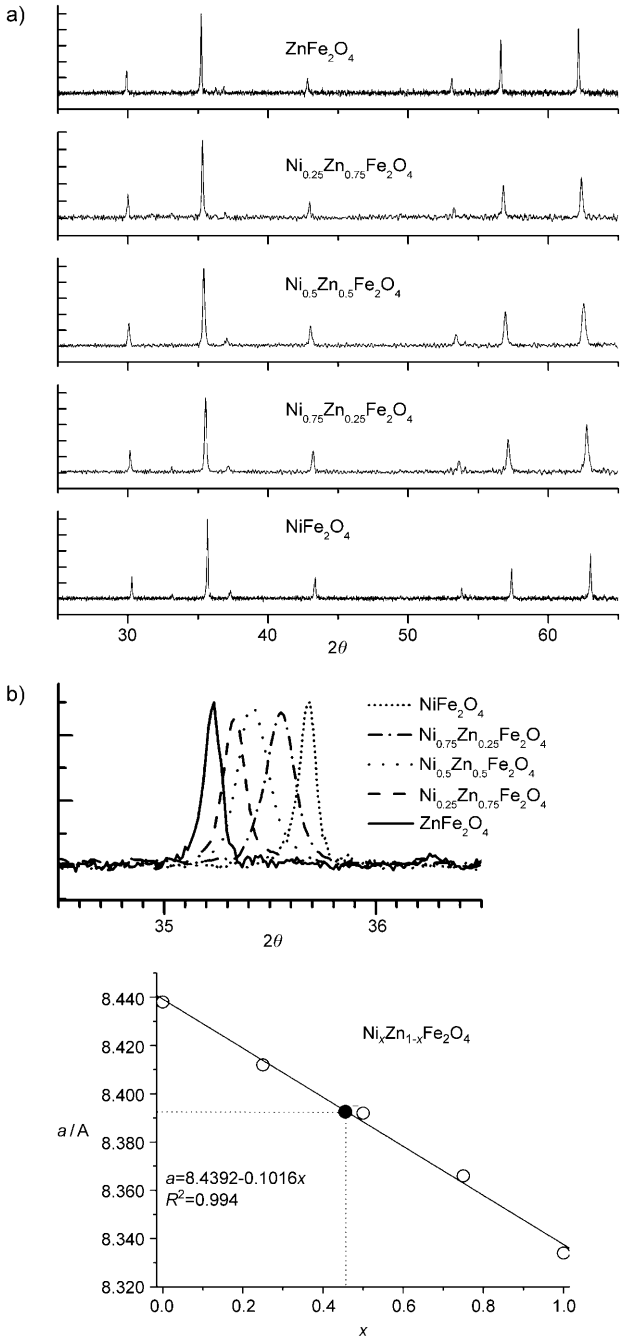

Figure 2. a) The effect of the Ni/Zn ratio on PXRD patterns. b) Shift of the reflection (311) and its linear dependence upon the amount of nickel in the ferrite core.

This effect is due to the increase in the crystallographic cell dimensions with decreasing Zn content.[19] Fitting the reflection shift by linear regression (Figure 2b) yielded the stoichiometry of the obtained mixed ferrite nanoparticles as $Ni_{0.465}Zn_{0.535}Fe_2O_4$; this is slightly different from expectations, yet within the experimental error both of the synthesis and of the diffraction experiments. Finally, a control experiment was carried out with two types of ferrite nanoparticles—$NiFe_2O_4$ and $ZnFe_2O_4$—mixed in 1:1 molar ratio. The

PXRD pattern (not shown) exhibits a set of double reflections, corresponding to the presence of the two separate phases in this mixture, in contrast with a single set of reflections (Figure 1) characterizing a single phase of mixed, nickel–zinc ferrite nanoparticles.

Nanoparticle sorting and sizing: Stock unsorted ferrofluid was diluted with aqueous TMAH solution (0.25%) to a final volume of 100 mL and a concentration of 24 mg mL^{-1}. Equivolume samples of this solution were centrifuged at 2500 *g* for 1 h, sediment was collected, and the supernatant was centrifuged again at 5000 *g*. The supernatant was sonicated for 10 min prior to each centrifuge run. This stepwise procedure was repeated at 7500 *g*, 10000 *g*, 13500 *g*, and finally at 18500 *g*, the latter for 2 h. The resultant pellets were washed several times with acetone and dried at 90 °C. The last clear supernatant, denoted from now on as SN > 18500 *g* for simplicity, was also precipitated and washed with acetone, and then dried at 90 °C. All samples were analyzed with a D8 Discover diffractometer (Bruker) with $Cu_{K\alpha}$ radiation. The resulting PXRD patterns are shown in Figure 3a. The data were then analyzed with the aid of Topas3 software to determine the average crystallite size in each fraction. Before analysis of peak broadening due to the nanocrystalline structures of the samples, the instrument broadening functions were determined by fitting the diffractogram of a silicon standard (NIST 640c). These parameters were fixed, and peak broadening for seven ferrite peaks in the 20–70° 2θ range was analyzed by the same routine.

The results of peak-profile fitting procedure are shown in Figure 3b. These data show that the relatively simple sorting method can be used to separate fractions containing nanoferrites of different diameters. However, it should be noted that these fractions are not monodisperse. Additionally, the diameters obtained with the Scherrer equation show only the crystalline cores of nanoparticles, which can have some amorphous shell increasing their real size. It should also be noted here that comparison of various fitting routines (e.g., FWMH and integral breadth (IB)) shows that FWMH yields slightly higher average particle radius values than the IB procedure. The average nanoparticle size data shown in this work are for the FWMH routine.

Surface modification of mixed nanoferrites: The resulting FTIR spectra of nanoferrites grafted with oleic acid are shown in Figure 4a. This Figure also shows the spectra of free oleic acid (Figure 4b) and unmodified particles (Figure 4c).

There are several diagnostic regions that confirm the surface grafting. The first region shows two peaks at 2920 cm^{-1} and 2850 cm^{-1} corresponding to stretching vibrations of methylene groups: asymmetric and symmetric, respectively. The band at 2960 cm^{-1} corresponds to the asymmetric stretching vibration of the methyl group. The strong band at ca. 1710 cm^{-1}, related to the stretching vibration of carbonyl groups of free oleic acid, is greatly diminished upon grafting and shifted towards lower wavenumbers. The presence of

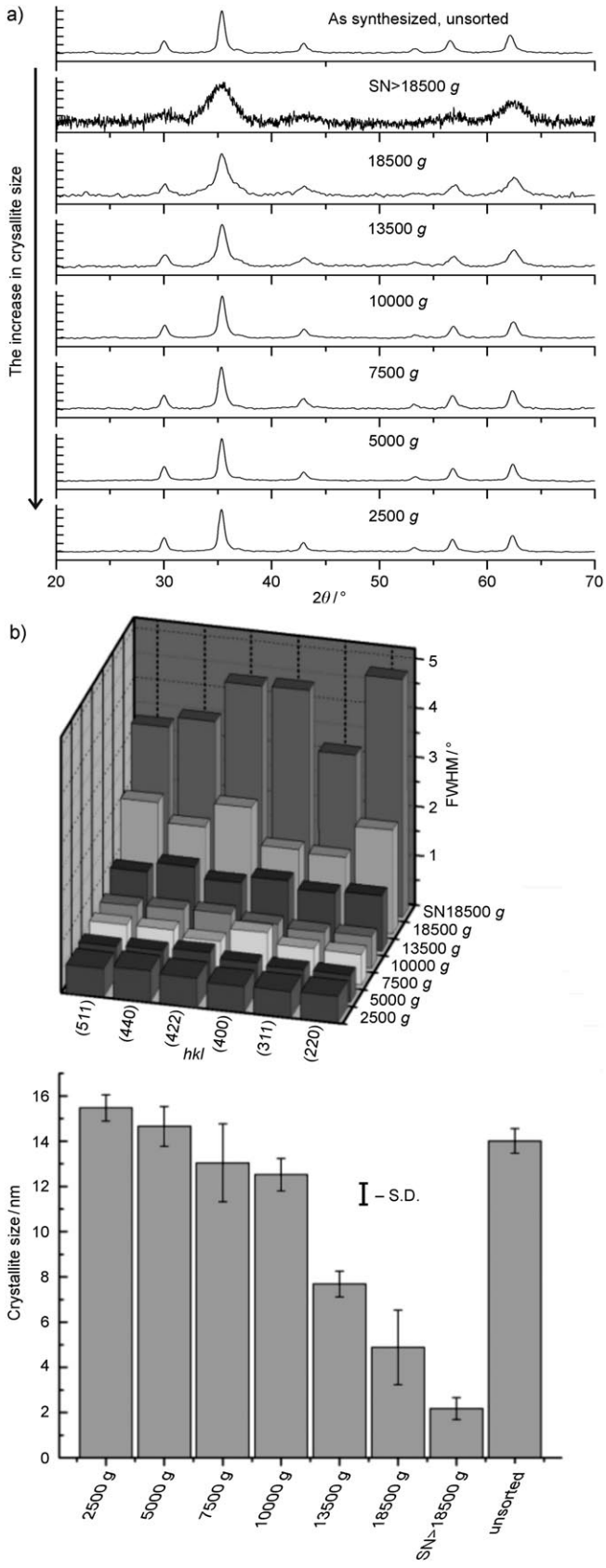

Figure 3. a) PXRD patterns of fractioned nanoferrites. b) Peak profile fitting and the resultant mean diameters of nanoparticles in each fraction. S.D. = standard deviation.

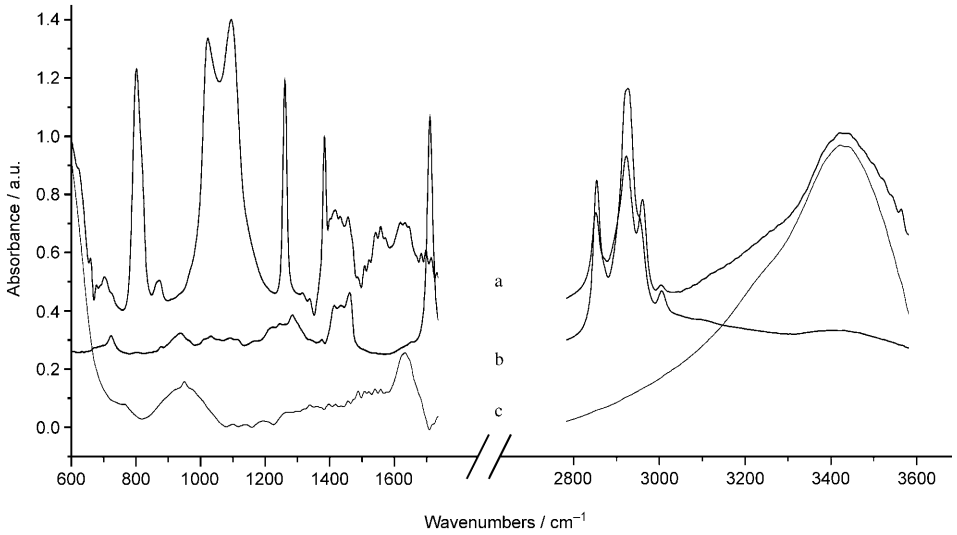

Figure 4. FTIR spectra (diagnostic regions) of a) nanoferrites grafted with oleic acid, b) free oleic acid, and c) unmodified nanoparticles.

several overlapping bands between 1500 cm^{-1} and 1650 cm^{-1}, as well as at 1300–1450 cm^{-1}, suggests the formation of a condensation product of the reaction between the hydroxylated nanoferrite surface and the oleic acid.[25,30] The broad band in the 3000–3500 cm^{-1} range is due to the presence of surface-bound −OH functionalities on the nanoparticle surface.

FTIR spectra for the nanoferrites modified with adipoyl chloride or sebacoyl chloride are shown in Figure 5.

Analysis of the diagnostic regions confirms the formation of an adlayer on the hydroxylated nanoparticle surface. There are no observable methyl group vibrations; only methylene group stretching vibrations at 2850 cm^{-1} and 2930 cm^{-1} are visible. The acid chloride C=O peak characteristic for an unbound molecule around 1810 cm^{-1} decreases coincidently with the appearance of ester C=O resonances at 1748 cm^{-1}. The presence of several bands between 1400 cm^{-1} and 1650 cm^{-1} is also associated with the symmetric and asymmetric stretches of a terminal carboxylate. These data indicate the hydrolysis of the terminal acid chloride moiety. The FTIR spectrum also contains ester-like stretches at 1046 cm^{-1} (widening of this band is most probably due to overlapping with the C–H bending stretch at 1020 cm^{-1}) and 1260 cm^{-1}. The correspondence of these bands to those of esters demonstrates the formation of adipoyl or sebacoyl adlayers on the nanoferrite particles through ester-type C–O covalent bonds with the hydroxy functionalities present in abundance on the surfaces.[20]

Similarly to the adipoyl and sebacoyl spectra, the spectrum of nanoferrites modified with a palmitoyl adlayer (spectrum not shown) displays characteristics that can be ascribed to the formation of ester-type C–O bonds with hydroxy groups present on the particle surfaces.[20] The noticeable difference is in the 2800 cm^{-1}–3050 cm^{-1} range, where $-CH_3$ vibrations due to the methyl terminal groups of this particular adlayer are present. Moreover, there are no vibrations attributable to carboxylate groups.

Importantly, modification with adipoyl or sebacoyl adlayers makes the surfaces of mixed nanoferrites available for further synthetic tailoring by, for example, amide or ester bonding of desired chemicals. We therefore tested this availability by attaching aminopyrene molecules to the particles through amide bonds between the terminal acid chloride moieties of the adlayer and aminopyrene.

Figure 6 presents the resulting steady-state fluorescence spectra both of a suspension of nanoparticles in water (Figure 6a) and of dry nanoparticles deposited on quartz (Figure 6b). The emission spectra of modified nanoparticles are qualitatively similar to those reported for 1-amidopyrene hexanoate bound to ITO and silica

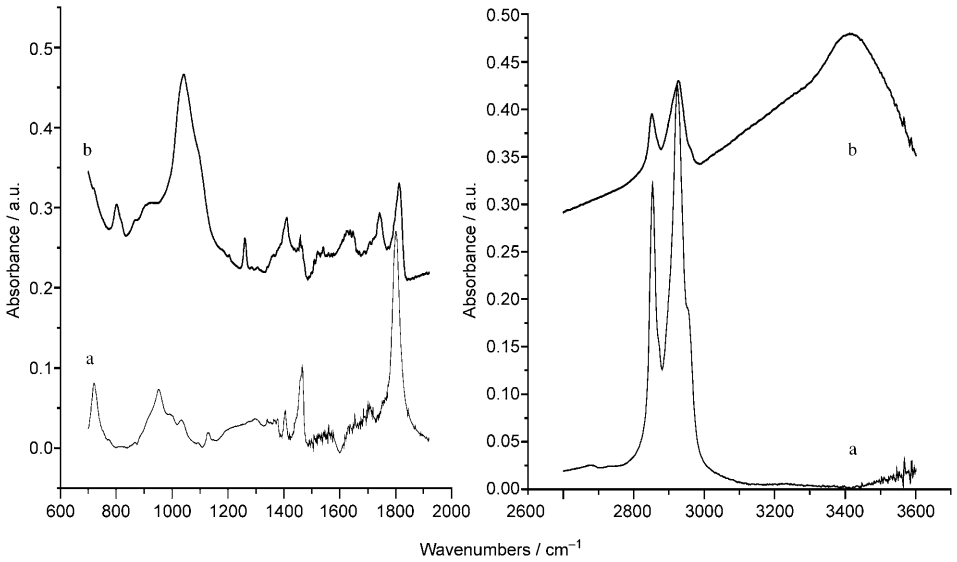

Figure 5. FTIR spectra (diagnostic regions) of a) free sebacoyl chloride, and b) nanoferrites grafted with sebacoyl chloride adlayer.

surfaces,[11,21] indicating that the nanoferrites are now decorated with this fluorophore. Steady-state spectroscopy on this system reveals the presence of excimers in the adlayer bound to the nanoferrite surface. The emission spectra (though most probably quenched[22]) of the chromophores bound to nanoferrites, both deposited on quartz and in the aqueous suspension, each show two small maxima, centered near 384 nm and near 405 nm. These maxima are each tailed with a broad shoulder to the red (particularly evident for dry nanoferrites deposited on quartz), in a spectral region where pyrene aggregates are known to emit. The presence of this shoulder and the absence of well-resolved spectral features in the vicinity of the emission maxima for both systems is consistent with excimer formation. We make this statement on the basis of our earlier work and of literature data.[11,12,23,24]

Monolayers of mixed nickel–zinc ferrite nanoparticles: A sample of organic ferrofluid grafted with oleic acid was diluted with the more volatile *n*-pentane to a final concentration of 5 mg mL^{-1}, as evaluated by VIS spectroscopy. This sample was used for Langmuir film formation, either on aqueous or aqueous ammonia (0.1 M) subphases.

The results, in the form of pressure/area (Π/A) isotherms, are shown in Figure 7. The insert shows control isotherms of oleic acid under the same experimental conditions.

This control experiment shows that the free oleic acid molecules do not form a monolayer on an NH_3 (0.1 M) subphase, being soluble in this alkaline subphase. In contrast, ferrite nanoparticles grafted with oleic acid can easily form Langmuir-type films both on aqueous and on aqueous ammonia (0.1 M) subphases. It has been reported in several works[25,26] that oleic acid adsorbs very strongly on magnetite

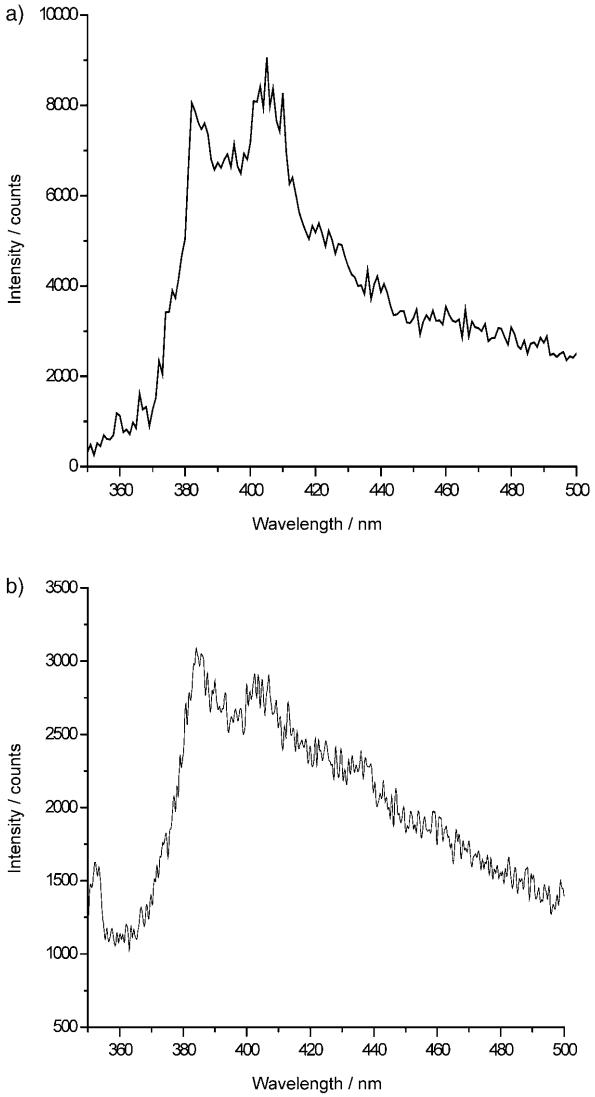

Figure 6. Steady-state emission fluorescence spectra of nanoferrites decorated with aminopyrene by acid chloride chemistry a) in aqueous suspension, and b) as a solid deposit on quartz in air. Excitation wavelength 320 nm.

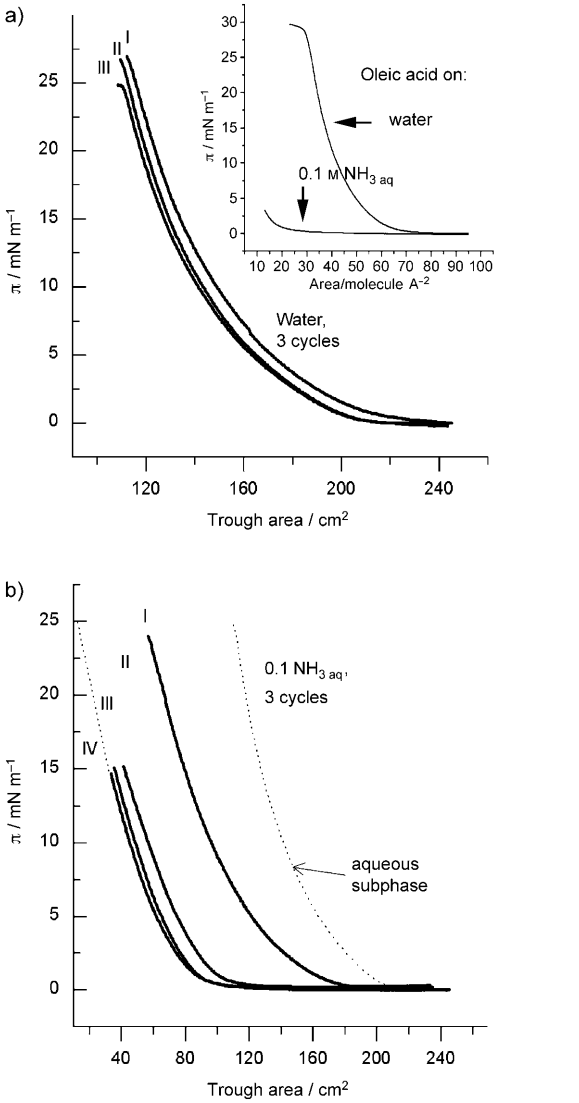

Figure 7. Langmuir isotherms of nickel–zinc nanoferrites grafted with oleic acid on water (curve a) and aqueous ammonia (0.1 M, curve b). The insert shows the Langmuir isotherms of oleic acid on these subphases, without nanoparticles.

and maghemite nanoparticles. Similar Langmuir isotherms of maghemite nanoparticles covered with lauric acid on an aqueous subphase have been reported.[27] There are, however, essential differences between the isotherms recorded on water and on NH_3 (0.1 M). The compression/decompression isotherm cycles on water are reproducible, while the same experiments carried out on ammonia (0.1 M) yield gradual shifts of subsequent compression isotherms towards lower areas of the trough until reproducible isotherms are obtained (Figure 7b, curves III and IV). This shift is due to desorption and dissolution of traces of unbound oleic acid. The reproducible isotherms were subsequently used to evaluate the diameters of the grafted nanoferrites, with the assumption of a densely packed 2D lattice of spherical particles and knowledge of the amount of nanoferrites (84 μg) and particle density (5.27 $g\,cm^{-1-3}$, from PXRD data). These evaluations yielded a value of mean particle diameter equal to (21 ± 3) nm. Subtraction of the doubled thickness of an oleic acid shell (in the all-*trans* hydrocarbon chain configuration) gives a value of (18 ± 3) nm, a value comparable to the mean diameter of unsorted particles obtained from PXRD data described above.

The same procedure was carried out for the organic ferrofluid covalently modified with palmitoyl monolayer. The resulting Langmuir isotherm (compression/decompression cycle) is shown in Figure 8.

This isotherm is qualitatively different from that obtained for oleic acid-grafted nanoferrites. It shows evidence of a liquid–solid phase transition at about 15 $mN\,m^{-1}$ with large hysteresis between the compression and decompression isotherms. This is because palmitoyl chains bound to nanoparticles are saturated, and therefore solid at the experimental temperature (21 °C). It is interesting to note that there is no collapse pressure recorded up to 50 $mN\,m^{-1}$, only a hump on the isotherm around 25 $mN\,m^{-1}$. We think that this might correspond to the overlapping of densely packed monolayer lattices one upon another, forming bilayer/multilayer structures of nanoferrites on the aqueous subphase. This observation is currently undergoing experimental verification. The part of the compression isotherm corresponding to the solid-like monolayer was used to evaluate the diameters of the palmitoyl-functionalized nanoferrites, as described above. These evaluations gave a value of mean grafted particle diameter equal to (13 ± 3) nm, corresponding to (10 ± 3) nm for the nanoferrite core—a value within the experimental error of the PXRD data.

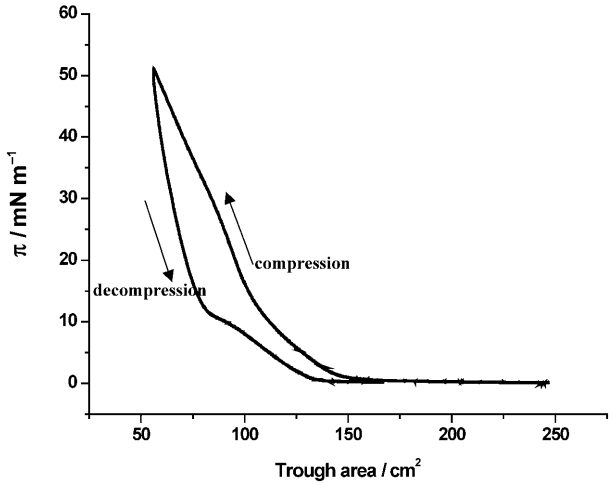

Figure 8. Compression/decompression cycle of mixed nanoferrites with covalently bound palmitoyl adlayer.

Conclusions

The synthesis, functionalization, and properties of magnetic nanoparticles have already attracted considerable interest in modern materials science. In this work we report on the covalent attachment of monomolecular adlayers to mixed nickel–zinc nanoferrite surfaces. Nanoferrites were subjected to surface modification by means of acid chloride chemistry, leading to the formation of covalent bonds between the hydroxy groups at the nanoparticle surfaces and acid chloride molecules. Herein we have used adipoyl and sebacoyl chlorides to functionalize the surfaces of nanoferrites. This procedure can be easily tailored to allow for the formation of adlayers containing both hydrophobic and hydrophilic regions stacked at predetermined distances from the magnetic core, and also providing the colloidal nanoferrites with functional carboxy groups capable of further modifications with, for example, drug molecules. Here, the fluorophore molecules of aminopyrene have been bound to such modified nanoferrites through amide bonds, and the steady-state fluorescence spectra have been recorded, confirming the fluorophore attachment.

We also used the same chemistry to modify the surfaces with covalently bound long-chain palmitoyl moieties, and for comparison we also modified the nanoferrite surfaces by simple adsorption of oleic acid. Both procedures made the surfaces highly hydrophobic. These hydrophobic, sterically stabilized colloids were subsequently spread on an aqueous surfaces to form Langmuir monolayers with totally different characteristics.

Since uniformity of size distribution is crucial in a number of practical applications, in this work we therefore also propose an efficient way of sorting nanoferrite particles by size. The colloidal suspension of nanoparticles is centrifuged at increasing rotational speed, and the fraction sedimented on the bottom of the centrifuge tube is collected after each run. Quantitatively, the mean size of nanoferrites in each fraction is measured by the powder X-ray diffraction (PXRD) technique.

Experimental Section

Materials: All chemicals were of the highest quality available commercially: $Fe(NO_3)_3{\cdot}9H_2O$ (p.a. Sigma), $Ni(NO_3)_2{\cdot}6H_2O$ (p.a., POCH, Poland), $Zn(NO_3)_2{\cdot}6H_2O$ (p.a., POCH, Poland), NaOH (p.a., POCH,

Poland), HNO_3 (p.a., POCH, Poland), tetramethylammonium hydroxide (TMAH, p.a., Sigma), oleic acid (pure, POCH, Poland), adipoyl chloride (Aldrich, 98%.), sebacoyl chloride (Aldrich, 99%), palmitoyl chloride (Aldrich, 98%), acetonitrile (dry, Aldrich, 99.8%), chloroform (p.a., Chempur), 4-methylmorpholine (Aldrich, 99%), sym.-collidine (Fluka, $\geq$98%), and *n*-hexane (p.a., Merck). All solutions were prepared with milliQ® water.

Methods: synthesis and surface modification

Synthesis of mixed ferrite $Ni_{0.5}Zn_{0.5}Fe_2O_4$: In this work we describe nanoparticles of mixed nickel–zinc ferrite of general formula $Ni_{0.5}Zn_{0.5}Fe_2O_4$. To verify the mixed behavior of such ferrites (as opposed to mixtures of nickel and zinc ferrites), we performed PXRD experiments with controlled samples of nickel, zinc, and mixed ferrite.

Mixed nickel–zinc ferrites were prepared by the "bottom-up" technique by co-precipitation of nanoferrites from a solution of their precursors with strong base. The method used is derived from that originally proposed by Massart[28] and theoretically described by LaMer.[29] This theory predicts that large, local oversaturation is required to obtain small nanoparticles.

The synthesis was carried out by mixing a heated aqueous solution of nickel, zinc, and iron salt with a hot aqueous solution of sodium hydroxide. Generally, in ionic form, this can be written as given in Equation (1):

$$Ni^{2+}+Zn^{2+}+4\,Fe^{3+}+16\,OH^- \rightarrow 2\,Ni_{0.5}Zn_{0.5}Fe_2O_4\downarrow+8\,H_2O \quad (1)$$

It is crucial to maintain the reaction temperature above 80 °C since below this temperature the resultant hydroxides do not undergo dehydration to form mixed ferrite oxides.

The crude precipitate consists of highly coagulated, roughly spherical nanoparticles of diameter dependent on the reaction conditions. In this work, the reaction mixture contained: Fe^{III} (0.6667 M), Ni^{II} (0.1667 M), and Zn^{II} (0.1667 M), prepared from their respective precursor salts.

The precursor solution (40 mL), acidified with HNO_3 (2 M, 8 mL) and water (152 mL), was heated to 95 °C under reflux with continuous stirring. An aqueous solution of NaOH (3 M, 100 mL), diluted with water (300 mL), was preheated to 95 °C in a separate container. The amount of NaOH was adjusted such as to obtain a final concentration of 0.3 M after precipitation of mixed ferrites and neutralization of HNO_3. The NaOH solution was then poured rapidly into the reaction vessel, with vigorous stirring. The resultant dark brownish precipitate was left heated for the next 12–16 h with stirring. Then, after the system had cooled to room temperature, the obtained coagulated nanoparticles (NPs) were precipitated with the aid of a magnet and clear supernatant was decanted. The precipitate was washed three times with deionized water (200 mL) with sedimentation in the field of a magnet and decantation. Total desorption of adsorbed, screening sodium ions was effected by addition of HNO_3 (2 M, 100 mL) and brief stirring. The precipitate was separated as above and washed twice with deionized water (100 mL). The resultant colloidal suspension was subsequently coagulated by increasing the pH to 6.5–7.5 with small amounts of tetramethylammonium hydroxide (TMAH) solution. Further TMAH solution (25%, 0.5 mL) was then added to the brown precipitate, and the system was thoroughly mixed to yield a deeply dark brown dense fluid (20 mL, 150 mg mL^{-1} of mixed nickel–zinc ferrite, pH 12.5) that could be attracted by a magnet without phase separation. The ferrofluid concentration was evaluated by visible absorbance at 500 nm. A calibration curve of absorbance versus a known amount of dry mixed ferrites per unit volume was used. A linear relationship (R^2= 0.998) of absorbance versus concentration was obtained within the range of 0.05 mg mL^{-1} to 0.5 mg mL^{-1} of dry ferrites.

Grafting with oleic acid: Surface modification of ferrite nanoparticles was carried out by adapting the procedure described in the literature.[30] Briefly, ferrofluid solution containing nanoparticles (200 mg) was diluted with water (20 mL), with subsequent addition (with stirring) of nitric acid (2 M) to pH 2.2. Nanoparticles were flocculated with $NH_{3\,aq.}$ (0.5 M) to pH 6.5–7.0. The precipitate was washed several times with water, facilitating phase separation with a magnet. The nanoparticles were then resuspended in water (20 mL) in contact with oleic acid (1 mL). After vigorous shaking (5 min) all magnetic material had been transferred to the organic phase. The aqueous phase was discarded, and the organic phase was extracted twice with a methanol/water mixture (3:1 v/v, 10 mL) to remove the excess of oleic acid. Finally, to remove the unbound oleic acid, the organic ferrofluid was washed with $NH_{3\,aq.}$ (0.1 M, 10 mL) in a methanol/water mixture to form the ammonium salt of unbound oleic acid. This was extracted with a methanol/water mixture (3:1 v/v, 10 mL). The procedure yielded a intensively colored dark brown organic ferrofluid in *n*-hexane, resembling the starting aqueous sample. A sample of this ferrofluid was dried, washed with acetone, dried again, and mixed with dry KBr. A tablet was formed, and FTIR spectra were recorded.

Grafting with alkyl acid chlorides: While several methods to endow nanoparticles with various functionalities suitable for—for example—biological applications have been proposed,[5,9,15] here we propose a simple acid chloride chemistry strategy for the modification of nanoferrite surfaces. Such chemistry can be used on different surfaces, both metallic and nonmetallic, with the proviso of the presence of a hydroxide layer on such surfaces.[12,20] Moreover, the adlayer moiety formed can be tailored with respect to structure and thickness by use of appropriate chemistry. The presence of the reactive acid chloride terminal functionality provides an efficient and robust means for binding a variety of species. In this work, a sample of ferrofluid (20 mg nanoparticles) was flocculated and washed several times with acetone, separated, and dried. This dried sample was suspended in dry acetonitrile (10 mL) under nitrogen. Adipoyl, sebacoyl, or palmitoyl chloride (depending on the desired modification) was added to this sample, together with 4-methylmorpholine (collidine in the case of palmitoyl chloride) as a Lewis base (final volume ratio 50:1:1, v/v/v). The resulting mixture with suspended ferrites was stirred under nitrogen for about 1 h. The ferrite particles were then precipitated with the aid of a magnet, and the reaction mixture was discarded. The precipitate was washed several times with an abundance of acetonitrile and then with acetone, and was then dried. Subsequently it was mixed with dry KBr, a tablet was formed, and FTIR spectra were recorded. The sample of nanoferrites modified with palmitoyl chloride was resuspended in chloroform to a final concentration of 11.3 mg mL^{-1}, yielding an organic ferrofluid stabilized sterically by the palmitoyl adlayer covalently bound to the surface of nanoparticles.

Surface modification with fluorophore: Surface modification with fluorophore was adapted from the procedure described elsewhere.[11,12] Ferrite particles freshly modified with sebacoyl chloride, after the reaction mixture had been discarded, were washed in the reaction vessel (while under nitrogen) several times with an abundance of dry acetonitrile and resuspended in this solvent (10 mL). A dry acetonitrile solution of aminopyrene (1 mM) was added to this suspension by cannula, followed by 4-methylmorpholine as a Lewis base (final volume ratio 50:1:1, v/v/v). The resultant mixture was stirred under nitrogen for about 2 h. The ferrite particles were then precipitated with the aid of a magnet, and the reaction mixture was discarded. The precipitate was washed several times with an abundance of acetonitrile and then with acetone, and was then dried. Steady-state fluorescence spectra were recorded after the nanoparticles were suspended in water. Additionally, the fluorescence spectra were recorded for the supernatant for traces of unbound aminopyrene.

Characterization methods: Powder X-Ray Diffraction (PXRD) experiments were carried out on a D8 Discover powder diffractometer (Bruker) with use of $Cu_{K\alpha}$ radiation. Diffractograms were recorded for 2θ from 20° to 70° at a scan rate of 1° min^{-1} in 0.012° steps. The results were analyzed and fitted with the aid of pseudo-Voight functions and the Topas program (Bruker) and compared against the ICDD database.[31] The PXRD instrument was situated at the Surface Research Laboratory, Department of Chemistry, University of Warsaw. Langmuir and Langmuir–Blodgett experiments were carried out in a NIMA 611 M trough (NIMA Techn., UK). Steady-state emission spectra were recorded with a Jobin–Yvon Fluorolog 3 (with TCSPC option) spectrometer with use of a 5 nm band-pass for excitation and a 5 nm band-pass for emission collection. FTIR spectra were recorded with a Shimadzu FTIR 8400/SSU 8000 spectrometer, with 2 cm^{-1} resolution.

Acknowledgements

PXRD measurements were carried out at the Structural Research Laboratory (SRL), Chemistry Department, Warsaw University, Poland. The SRL was established with financial support from the European Regional Development Fund in the Sectoral Operational Programme "Improvement of the Competitiveness of Enterprises, years 2004–2006" project no: WKP_1/1.4.3./1/2004/72/72/165/2005/U.

[1] T. Tsutaoka, *J. Appl. Phys.* **2003**, *93*, 2789.
[2] D. I. Leslie-Pelecky, R. D. Rieke, *Chem. Mater.* **1996**, *8*, 1770.
[3] H. Hartshorne, C. J. Backhouse, W. E. Lee, *Sens. Actuators B* **2004**, *99*, 592.
[4] B. T. Naughton, P. Majewski, D. R. Clarke, *J. Am. Ceram. Soc.* **2007**, *90*, 3547.
[5] A. N. Shipway, I. Willner, *Chem. Commun.* **2001**, 2035.
[6] G. Schneider, G. Decher, *Nano Lett.* **2004**, *4*, 1833.
[7] Y. Jun, Y.-M. Huh, J. Choi, J.-H. Lee, H.-T. Song, S. Kim, S. Yoon, K.-S. Kim, J-S. Shin, J. S. Suh, J. Cheon, *J. Am. Chem. Soc.* **2005**, *127*, 5732.
[8] J. S. Kim, W. J. Rieter, K. M. L. Taylor, H. An, W. L. Lin, W. B. Lin, *J. Am. Chem. Soc.* **2007**, *129*, 8962.
[9] C. Grüttner, K. Müller, J. Teller, F. Westphal, A. Foreman, R. Ivkov, *J. Magn. Magn. Mater.* **2007**, *311*, 181.
[10] T. Neuberger, B. Schöpf, H. Hofmann, M. Hofmann, B. von Rechenberg, *J. Magn. Magn. Mater.* **2005**, *293*, 483.
[11] L. Kelopouris, P. Krysiński, G. J. Blanchard, *J. Phys. Chem. B* **2003**, *107*, 4100.
[12] P. Krysinski, G. Blanchard, *Langmuir*, **2003**, *19*, 3875.
[13] P. Krysiński, Y. Show, J. Stotter, G. J. Blanchard, *J. Am. Chem. Soc.* **2003**, *125*, 12726.
[14] L. Machala, R. Zboril, A. Gedanken, *J. Phys. Chem. B* **2007**, *111*, 4003.
[15] K. R. Reddy, K.-P. Lee, A.-G. Iyengar, *J. Appl. Polym. Sci.* **2007**, *104*, 4127.
[16] E. A. Souza, J. G. S. Duque, L. Kubota, C. T. Meneses, *J. Phys. Chem. Solids* **2007**, *68*, 594.
[17] R. C. Woodward, J. Heeris, T. G. St. Pierre, M. Saunders, E. P. Gilbert, M. Rutnakornpituk, Q. Zhang, J. S. Riffle, *J. Appl. Crystallogr.* **2007**, *40*, s495.
[18] S. Lefebure, E. Dubois, V. Cabuil, S. Neveu, R. Massart, *J. Mater. Res.* **1998**, *13*, 2975.
[19] S. Morrison, C. L. Cahill, E. E. Carpenter, S. Calvin, R. Swaminathan, M. E. McHenry, V. G. Harris, *J. Appl. Phys.* **2004**, *95*, 6392.
[20] P. Krysiński, G. J. Blanchard, *Bioelectrochemistry* **2005**, *66*, 71.
[21] M. Dominska, P. Krysinski, G. J. Blanchard, *J. Phys. Chem. B* **2005**, *109*, 15822.
[22] N. J. Turro, P. H. Lakshminarasimhan, S. Jockusch, S. P. O'Brien, S. Grancharov, F. X. Redi, *Nano Lett.* **2002**, *2*, 325.
[23] C. E. Kerr, C. D. Mitchell, J. Headrick, B. E. Eaton, T. L. Netzel, *J. Phys. Chem. B* **2000**, *104*, 1637.
[24] C. D. Mitchell, T. L. Netzel, *J. Phys. Chem. B* **2000**, *104*, 125.
[25] M. Klokkenburg, J. Hilhorst, B. H. Erné, *Vib. Spectrosc.* **2007**, *43*, 243.
[26] K. Butter, A. Hoell, A. Wiedenmann, A. V. Petukhov, G.-J. Vroege, *J. Appl. Crystallogr.* **2004**, *37*, 847.
[27] S. Lefebure, C. Menager, V. Cabuil, M. Assenheimer, F. Gallet, C. Flament, *J. Phys. Chem. B* **1998**, *102*, 2733.
[28] R. Massart, *IEEE Trans. Magn.* **1981**, *17*, 1247.
[29] V. K. LaMer, R. H. Dinegar, *J. Am. Chem. Soc.* **1950**, *72*, 4847.
[30] G. A. van Ewijk, G. J. Vroege, A. P. Philipse, *J. Magn. Magn. Mater.* **1999**, *201*, 31.
[31] International Center for Diffraction Data, Pennsylvania, USA, **1995**.

Received: February 29, 2008
Published online: July 11, 2008

